

# Synthesis and characterization of a new structure of gas hydrate

L. Yang<sup>a,b</sup>, C. A. Tulk<sup>a,1</sup>, D. D. Klug<sup>c</sup>, I. L. Moudrakovski<sup>c</sup>, C. I. Ratcliffe<sup>c</sup>, J. A. Ripmeester<sup>c</sup>, B. C. Chakoumakos<sup>a</sup>, L. Ehm<sup>d</sup>, C. D. Martin<sup>e</sup>, and J. B. Parise<sup>d</sup>

<sup>a</sup>Neutron Scattering Science Division, Oak Ridge National Laboratory, Oak Ridge, TN 37831; <sup>b</sup>Center of Nanophase Materials Science, Oak Ridge National Laboratory, Oak Ridge, TN 37831; <sup>c</sup>Steacie Institute for Molecular Sciences, National Research Council of Canada, Ottawa, ON, Canada K1A 0R6; <sup>d</sup>Mineral Physics Institute, Department of Geosciences, Stony Brook University, Stony Brook, New York, NY 11794; and <sup>e</sup>X-ray Sciences Division, Advanced Photon Source, Argonne National Laboratory, Argonne IL 60439

Edited by Ho-kwang Mao, Carnegie Institution of Washington, Washington, DC, and approved January 26, 2009 (received for review September 23, 2008)

**Atoms and molecules <0.9 nm in diameter can be incorporated in the cages formed by hydrogen-bonded water molecules making up the crystalline solid clathrate hydrates. For these materials crystallographic structures generally fall into 3 categories, which are 2 cubic forms and a hexagonal form. A unique clathrate hydrate structure, previously known only hypothetically, has been synthesized at high pressure and recovered at 77 K and ambient pressure in these experiments. These samples contain Xe as a guest atom and the details of this previously unobserved structure are described here, most notably the host-guest ratio is similar to the cubic Xe clathrate starting material. After pressure quench recovery to 1 atmosphere the structure shows considerable metastability with increasing temperature ( $T < 160$  K) before reverting back to the cubic form. This evidence of structural complexity in compositionally similar clathrate compounds indicates that the reaction path may be an important determinant of the structure, and impacts upon the structures that might be encountered in nature.**

high pressure | ice | clathrate hydrate

Clathrate hydrates are crystalline inclusion compounds composed of water molecules hydrogen-bonded to form cages of several types that, when stacked together, fill 3-dimensional space. Most hydrates belong to 3 structural families, 2 cubic forms known as sI and sII (1), and one hexagonal form known as sH (2–4). Species such as Ar, Kr, Xe and methane form sI or sII hydrate, whereas sH is unique in that it requires all types of cages (both small and large) to contain guest species for lattice stability (5). All 3 structures, containing methane, other hydrocarbons, H<sub>2</sub>S and CO<sub>2</sub>, O<sub>2</sub> and N<sub>2</sub> have been found in the geosphere, with sI methane hydrate by far the most abundant. At high pressures ( $P > 0.7$  kbar) small guests (Ar, Kr, Xe, methane) are also thought to form sH hydrate with multiple occupancy of the largest cage in the hydrate (6–8). It has been proposed that the high-pressure methane hydrate of sH plays a role in the outer solar system, including formation models for Titan (9, 10).

From a global perspective, natural gas clathrate hydrates are seen as a major energy resource, a potential climate change material and as a geohazard. In the natural gas industry, the prevention of gas hydrate blockages in pipelines is a major concern. From a climate change perspective the decomposition of natural gas hydrate can release large amounts of methane into the atmosphere, but paradoxically hydrates also have a potential for sequestration of anthropogenic greenhouse gases. Furthermore, clathrate hydrates have been explored for hydrogen storage.

In standard hydrate notation (where D = dodecahedral, T = tetrakaidecahedral, P = pentakaidecahedral, H = hexakaidecahedral, and E = eicosahedral; and for example  $5^{12} = 12$  5-sided faces), each of the cubic structures are made up of small and large water cages denoted as D( $5^{12}$ ) and T( $5^{12}6^2$ ) for sI (D<sub>2</sub>T<sub>6</sub> · 46 H<sub>2</sub>O); and D( $5^{12}$ ) and H( $5^{12}6^4$ ) for sII (D<sub>16</sub>H<sub>8</sub> · 136 H<sub>2</sub>O); whereas the hexagonal form is made up of 3 cages denoted

as small, D( $5^{12}$ ), medium, D'(4<sup>3</sup>5<sup>6</sup>6<sup>3</sup>), and large, E( $5^{12}6^8$ ) (D<sub>3</sub>D<sub>2</sub>E<sub>1</sub> · 34 H<sub>2</sub>O). Beside sI, II and H, other clathrate hydrate structures are known, for example those of bromine, *t*-butylamine and dimethyl ether. As well, several hypothetical structures have been postulated by Jeffrey and Dyadin (1, 11), based on known ionic or semiclathrate hydrates. However, true clathrate hydrates include only those compounds for which there are only weak van der Waals guest-host interactions.

For many years it was thought that hydrate structures were predictable, phase equilibrium can be predicted based on simple guest size-structure relationships and computational modeling. Some structural complexity in the clathrate hydrates is by now a well-recognized phenomenon, even to the extent that it is sometimes impossible to predict the structure(s) that will appear for a certain combination of guests (5). However, the observation here of 2 structurally distinct but compositionally similar and stable hydrates increases the importance of understanding complexity in these systems.

The low pressure form of sH hydrate is uniquely different from the other known structures that can be made with a single guest type in that it requires small “help gas” atoms or molecules to fill the small cages, and a large guest molecule to fill the large cage. However, at high pressure the sH phase forms for single types of small guest species (see below for more details) (7–9), along with the formation at still higher pressure of a nonclathrate form related to ice Ih with guest atoms filling its open channels, this form has been identified and called a filled ice structure (12). These can be made by the compression of the corresponding simple sI or sII hydrates. Apparently, this results in a reconstruction of the crystal lattice with multiple guests filling and stabilizing the large cage of sH.

In this study, we investigate the Xe clathrate hydrate system and demonstrate the formation of a hydrate structure not previously observed. As a result we now demonstrate 2 distinct crystallographic structures with very similar guest:host ratios, and 1 guest atom per cage, that are stable under similar conditions of temperature and pressure. Samples of the sI form xenon hydrate were compressed at room temperature for the in situ characterization of the resulting high pressure sH structure. Samples of the new phase resulted from pressure quench recovery at low temperature (77 K) to atmospheric pressure. Two such recovered samples were synthesized and studied by NMR (NMR) and X-ray diffraction techniques, including studies of

Author contributions: C.A.T., D.D.K., J.A.R., and J.P. designed research; L.Y., C.A.T., D.D.K., I.L.M., C.I.R., J.A.R., L.E., and D.M. performed research; L.Y., I.L.M., C.I.R., and B.C.C. analyzed data; and C.A.T., D.D.K., C.I.R., and J.A.R. wrote the paper.

The authors declare no conflict of interest.

This article is a PNAS Direct Submission.

Freely available online through the PNAS open access option.

<sup>1</sup>To whom correspondence should be addressed. E-mail: tulkca@ornl.gov.

This article contains supporting information online at [www.pnas.org/cgi/content/full/0809342106/DCSupplemental](http://www.pnas.org/cgi/content/full/0809342106/DCSupplemental).

the ambient pressure stability with increasing temperature and the decomposition path back to water and xenon gas. (See *Materials and Methods* for details of sample synthesis and details of the X-ray and NMR analysis).

## Results

The X-ray diffraction patterns and Rietveld refinements of lattice constants, guest occupancies (giving the water to guest ratio), host lattice oxygen and guest atomic positions, and displacement parameters are shown in Fig. 1A and Table 1. The upper 2 plots, collected at ambient pressure and 40 K and at 300 K and 1.7 GPa, respectively, represent the well-known Xe sI clathrate hydrate. The cage occupancy is refined to  $\approx 80\%$  for both cages giving a host-to-guest ratio of 7.06:1 (this ratio is assumed to be maintained for the fit to the sI form at higher pressure, 1.7 GPa), the lattice constants are observed to decrease with increasing pressure, as expected. Other details of the fit are given in Table 1.

The data collected at 300 K and 2.0 GPa are fitted well by parameters for sH plus  $\approx 5\%$  residual sI hydrate as determined from diffraction intensity ratios. The initial oxygen positions for the in situ high pressure sH fits were obtained from reference 3, with initially 1 atom in each small cage and 2 in the large cage (based on cage size). The fit converges nicely with an  $R_{wp} = 2.1\%$ , we have taken this to be a good fit and the fitted parameters are given in Table 1. At 2.0 GPa, not all of the sample had transformed to sH. Additionally, the fitted occupancy of the cages drops and lowers the host to guest ratio to 6.49:1, because this sample in its low pressure sI form originally contained 7.06:1 water to guest ratio (as determined for the fits discussed above) and that no solid Xe is observed, excess water is likely mixed with the sH sample in the pressure chamber.

Although it is not the main thrust of this article, there has been some discussion in the literature over the assignment of sH as the high pressure form. Originally the structure was thought to be closely related to, but not exactly, the sH form even though the lattice parameters were similar (9, 13). At the time this high pressure transformation was supported by a structure implied by Raman spectroscopic studies (14), although they conclude that at high pressure the structure is sH. At approximately the same time, Sanloup et al. (15) reported loading a diamond anvil cell (DAC) with water and Xe, and with energy dispersive X-ray diffraction data suggested an indexing consistent with a tetragonal space group. Indexing our in situ high pressure data does not provide a possible structure that is consistent with that reported by Sanloup. Later, Loveday et al. (8) revisited the diffraction work and subsequently corrected the occupancy of the large cavities of the high pressure form and showed that acceptable fits of the low pressure sH structure to the high pressure data are in fact achieved. This conclusion was further supported by follow-on experiments of the structure of argon hydrate by Ogienko et al. (7) Our data collected at 2.0 GPa in a DAC and reported herein build on this later interpretation and support the evidence indicating formation of the sH structure at high pressure.

The data obtained at 40 K after quenching the sample at 2.0 GPa to 77 K, followed by pressure release to ambient, are shown in the bottom plot of Fig. 1A. Fitting this data with a mixture of the sH form, found at high pressure, and the initial sI form gives an  $R_{wp} = 20\%$ , thus is a poor fit, and does not adequately reproduce the position of lowest angle (100) reflection of the recovered form. Subsequent refinement of the lattice constants and the peak widths modestly improves the quality of the fit with an  $R_{wp} = 15\%$ . However, a Le Bail fit with space group  $P6/mmm$  produces a good result, ( $R_{wp} = 2\%$ ), but with lattice parameters,  $a = 11.99\text{\AA}$ ,  $c = 11.51\text{\AA}$ . Generally, the  $c/a$  ratio of the sH structure seems to fall between 0.83 and 0.86 whether the sample is at high pressure or not; a value of 0.96 was thought to be too large and reinforces the notion that sH was not the correct

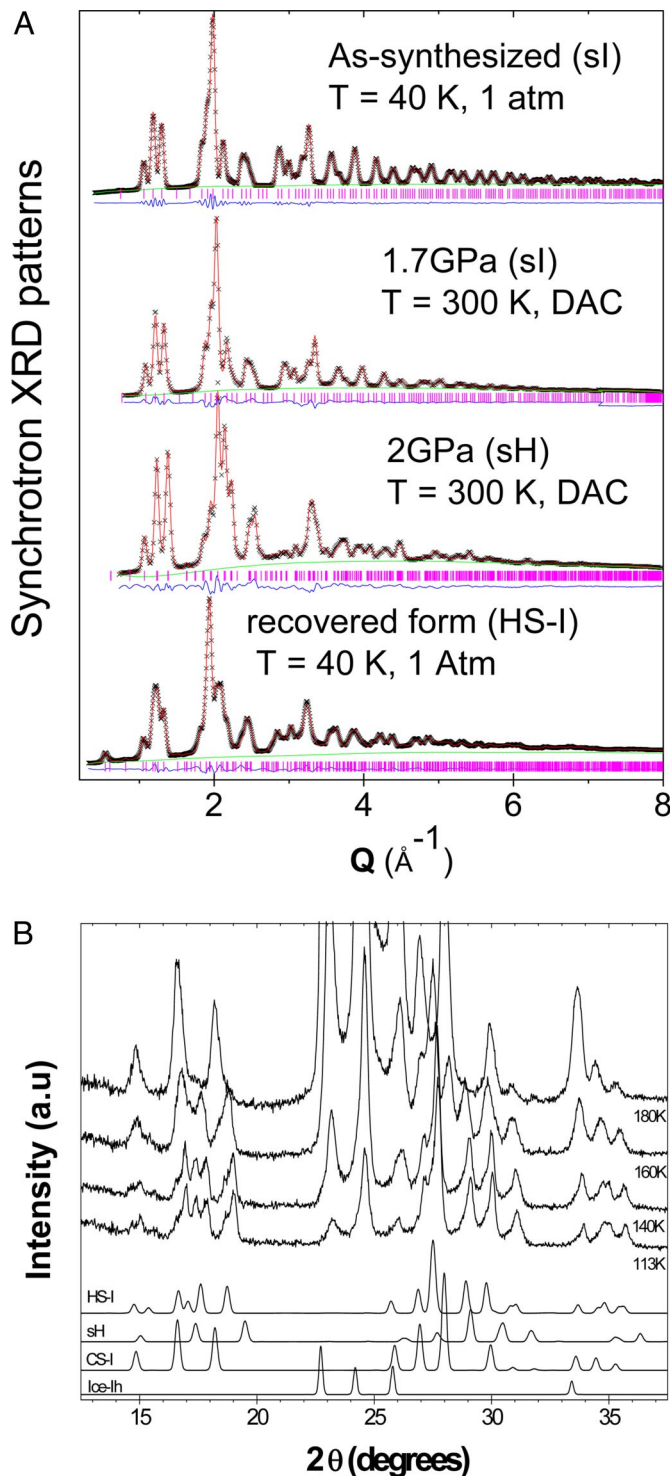


**Fig. 1.** X-ray diffraction data. (A) The sI form collected at 40 K; the in situ sI form at 1.7 GPa and room temperature; sH form at 2.0 GPa and room temperature; and the new quench-recovered HS-I form at ambient pressure and 40 K. (B) Decomposition of the quenched HS-I structure into ice I through the sI clathrate form.

structure of the recovered form. Furthermore, in this case spherical Xe atoms occupy all of the cages and we do not expect there to be any lowering of the crystallographic symmetry driven by cage distortion effects resulting from molecules of complex shapes, as seen recently by Udachin et al. (16) in the sH form at

**Table 1. Models and refined parameters for Xe clathrate**

Samples parameters	0 GPa 40 K		1.7 GPa RT		2.0 GPa RT			0 GPa 40K (Pressure-quenched)		
	sl ( <i>Pm</i> $\bar{3}$ n): 2D·6T·46H <sub>2</sub> O		sl ( <i>Pm</i> $\bar{3}$ n): 2D·6T·46H <sub>2</sub> O		sH ( <i>P6/mmm</i> ): 3D·2D'·1E·34H <sub>2</sub> O			HS-I <sub>Q</sub> ( <i>P6/mmm</i> ): 3D·2P·2T·40H <sub>2</sub> O		
Phase, space group, stoichiometry	sl ( <i>Pm</i> $\bar{3}$ n): 2D·6T·46H <sub>2</sub> O		sl ( <i>Pm</i> $\bar{3}$ n): 2D·6T·46H <sub>2</sub> O		sH ( <i>P6/mmm</i> ): 3D·2D'·1E·34H <sub>2</sub> O			HS-I <sub>Q</sub> ( <i>P6/mmm</i> ): 3D·2P·2T·40H <sub>2</sub> O		
Lattice, Å	<i>a</i> = 11.857 (1)		<i>a</i> = 11.574 (3)		<i>a</i> = 11.759 (7), <i>c</i> = 10.101 (4)			<i>a</i> = 11.987 (1), <i>c</i> = 11.509 (2)		
Site occupancy	D	T	D	T	D	D'	E	D	P	T
	0.80 (1)	0.82 (1)	0.80	0.82	0.74 (2)	0.69 (1)	1.64 (1)	0.80 (1)	0.87 (1)	0.79 (1)
H <sub>2</sub> O:Xe	7.06:1		7.06:1		6.49:1			6.99:1		
O-O length, Å	2.71–2.77		2.65–2.70		2.65–2.78			2.69–3.00		

Notes: D (5<sup>12</sup>), D' (4<sup>3</sup>5<sup>6</sup>6<sup>3</sup>), T (5<sup>12</sup>6<sup>2</sup>), P (5<sup>12</sup>6<sup>3</sup>), E (5<sup>12</sup>6<sup>8</sup>); all samples originated from the initial 0 GPa uncompressed batch; 2.0 GPa data contains 5% sl [*a* = 11.43 (1) Å]; because the total amount of Xe in the system is constant and the structure does not change and guest migration between cages is unlikely, the guest to host ratio and cage occupancies for the sl samples at 1.7 GPa are taken from the zero pressure data, this assumption results in good fits. The *U*iso (Å<sup>2</sup>) for Xe in sl are 0.01, 0.01 for D and T cages, for sH are 0.04, 0.07, 0.15 for D, D', and E cages, and for HS-I are 0.01 0.03 0.04 for the D, P, and T cages.

low temperature with cyclo-octane as a guest in the large cages. Thus, a different but closely related structure must have been recovered.

Dyadin's HS-I structure (11), and Jeffrey's related Hexagonal-I structure (1), which were only inferred from packing of complete cages based on related known structures of polyalkylammonium salt hydrates (11) and the semiclathrate trimethylamine hydrate (17) provided a strong candidate structure (we adopt the HS-I label from here on for convenience). Subsequent Rietveld fits used the initial oxygen atom positions from Kosyakov et al. (18), which were postulated based on lattice energy calculations for the structure HS-I with the formula D<sub>3</sub>(5<sup>12</sup>)·T<sub>2</sub>(5<sup>12</sup>6<sup>2</sup>)·P<sub>2</sub>(5<sup>12</sup>6<sup>3</sup>)·40H<sub>2</sub>O (18) and, based on cage size, only 1 Xe atom was located at the center of each cage. These results are shown in Fig. 1. Fitting a mixture of this HS-I plus the initial sl form provided a good overall fit with an *R*<sub>wp</sub> = 4%, resulted in good hydrogen bonded O–O distances, and a low sl fraction of only 2%. The residual sl is likely carried all of the way through from the initial starting material and results perhaps from pressure gradients, and the NMR data reported below cannot be used to determine the true phase fractions because it only gives the relative cage occupancies with each structure. The refinement of the guest occupancy resulted in a host to guest ratio that is similar to the original sl starting material. (See Table 1 for further information on the fitted parameters). The Br<sub>2</sub>·10H<sub>2</sub>O originally classified by Dyadin as HS-I was later shown by single crystal diffraction to be a different structure, tetragonal *P*4<sub>2</sub>/*mnn* (19), and not *P*6/*mmm* as are both the HS-I and sH forms and used in the Le Bail fit above. The same basic structure as HS-I also has appeared in a classical molecular dynamics simulation examining the transformation of methane clathrate hydrate from sl to sII (20).

The structural models for both hexagonal structures are plotted in Fig. 2. In the high pressure sH form, the large E(5<sup>12</sup>6<sup>8</sup>)

cages contain 2 Xe atoms located on the long axis of the cage, and the smaller D(5<sup>12</sup>) and D'(4<sup>3</sup>5<sup>6</sup>6<sup>3</sup>) cages contain 1 Xe atom each. The hydrogen bonds between the oxygen atoms around the waist of the large cage E(5<sup>12</sup>6<sup>8</sup>) in sH are shared by one edge of the D'(4<sup>3</sup>5<sup>6</sup>6<sup>3</sup>) cage, and these bonds make-up one side of the 4-membered hydrogen-bonded ring in the structure. It is reasonable to assume that these are the most strained bonds in the sH host lattice. Breaking these bonds and inserting a layer of water molecules changes the hexagons at the waist of the large E (5<sup>12</sup>6<sup>8</sup>) cage of sH into 2 pentagons of the T (5<sup>12</sup>6<sup>2</sup>) cages in HS-I. This results in the formation of 2 T (5<sup>12</sup>6<sup>2</sup>) cages containing only 1 Xe atom. Furthermore, it has also been predicted by molecular dynamics simulations that the optimum occupancy for this E (5<sup>12</sup>6<sup>8</sup>) cage is 2 Xe atoms (21). This further supports a suggestion that the repulsion of the 2 large cage Xe atoms initiates the formation of 2 separate T (5<sup>12</sup>6<sup>2</sup>) cages in the pressure quenched structure. The calculated mean Xe-Xe distance in the large cage is 4.19 Å at 40 K and 1 bar, where a Lennard–Jones potential is used for the Xe atoms. This means that the Xe atoms are well up on the repulsive side of the interatomic potential. In addition, if a Xe-Xe near-neighbor distance of 4.19 Å (21) is considered in the measured equation of state for solid Xe (22) the effective pressure for the Xe atoms is several kilobars and suggests that the large cages of sH may have a tendency to tear apart, because of strong repulsive forces between Xe atoms in the large cage, and form 2 smaller ones. This supports the suggestion of instability of the large cages in a high pressure sH clathrate upon recovery and that the formation of the new hexagonal structure with single occupancy cages is possible. This does not, however, rule out the possibility that the quenched structure could have formed as an intermediary between sl and sH.

This HS-I Xe hydrate shows a considerable range of metastability with respect to the sl cubic form at ambient pressure and low temperature. Fig. 1B shows laboratory powder X-ray diffraction (PXRD) data along with simulated patterns for ice Ih, sl clathrate and the quenched-recovered sample. The characteristic peaks for HS-I are prominent at 2θ ~ 30° and T < 160 K, with the transformation starting near 150 K. By 180 K the sample reverted to sl, before decomposing to ice I at 200 K. X-ray diffraction analysis indicates that the HS-I form is metastable during storage in liquid nitrogen for at least 3 months, however, the sl Xe hydrate structure does not transform to HS-I upon storage in liquid nitrogen. Molecular Dynamics simulations of this new structure indicate that the lattice is stable with respect to decomposition, at least on the timescale of the MD simulation, this will be reported in a subsequent article on the dynamics of this clathrate form.

Static and magic angle spinning (MAS) <sup>129</sup>Xe NMR spectra, Fig. 3, provide strong confirmation of the HS-I structural analysis. <sup>129</sup>Xe NMR chemical shifts are indicative of cage size

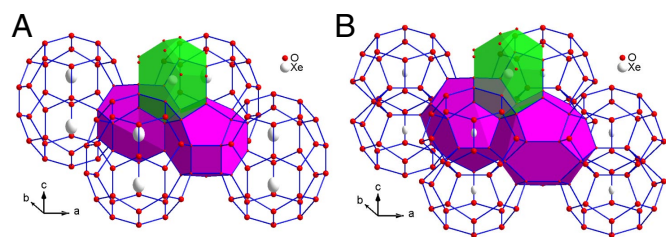


**Fig. 2.** Structure models fitted to high pressure sH (A) and the quenched-recovered HS-I (B) form. The green shaded cage represents the 5<sup>12</sup> polyhdera, the purple shaded cages are the 4<sup>3</sup>5<sup>6</sup>6<sup>3</sup> cage for sH; and the 5<sup>12</sup>, shaded green, and 5<sup>12</sup>6<sup>3</sup>, shaded purple, cages for the quenched HS-I form. The large 5<sup>12</sup>6<sup>8</sup> cage of the sH form is seen to contain 2 xenon atoms and this cage is divided into 2, each containing 1 xenon atom, in the quenched HS-I form.

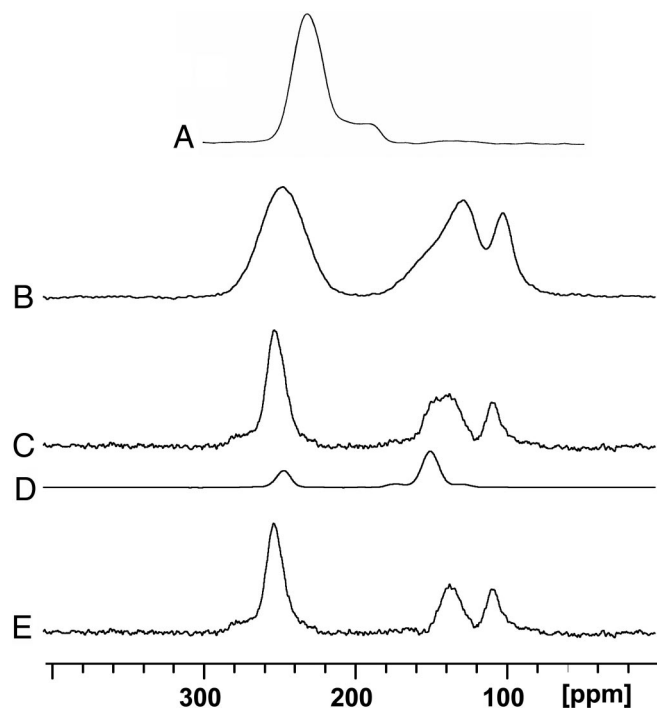


**Fig. 3.**  $^{129}\text{Xe}$  NMR spectra with  $^1\text{H}$  cross-polarization and decoupling. (A) Static sH hydrate of Xe/bicyclo[2.2.2]oct-2-ene at 77K (24). (B) Static quenched material at 77 K. (C) Quenched material at 153 K with MAS at 2.2 kHz. (D) Pure sI Xe hydrate at 153 K with MAS at 2.2 kHz. (E) Difference spectrum  $c-d \equiv \text{HS-I}$ . The Str.I spectrum (D) is scaled to show the intensity subtracted from spectrum C to give E. The shoulders on the 251 ppm line in C and E are spinning sidebands.

(larger shifts for smaller cages), and the chemical shift anisotropy (CSA) is sensitive to cage shape. Consequently different hydrate structures give quite distinct  $^{129}\text{Xe}$  spectra (23, 24). The static spectrum of HS-I at 77 K (Fig. 3B) does not correspond to any of the characteristic spectra of sI, sII or sH hydrates or combinations thereof. Furthermore, although the peak near 250 ppm in the  $^{129}\text{Xe}$  spectra of the quenched material corresponds to Xe in small cages it lacks the significant CSA characteristic of Xe in the D' ( $4^35^66^3$ ) cage of sH, thus ruling out the possibility that the quenched material contains sH with the other spectral lines corresponding to double occupancy of the large cage by Xe. A spectrum of a typical sH hydrate with Xe occupying only the smaller cages and a large molecule in the large cage is shown for comparison in Fig. 3A.

MAS at 153 K (Fig. 3C) removes broadening and shows isotropic shift resonances for Xe in the different cages. There are 2 overlapping lines in the 130–150 ppm region, of which the more shifted component corresponds to some remnant sI in the sample. If a scaled spectrum of sI (Fig. 3D) is subtracted, the spectrum of HS-I is revealed (Fig. 3E). The HS-I spectrum (difference spectrum) was obtained by subtracting increasing intensities of the sI spectrum to the extent that no distortions of the remaining peaks or negative peaks were obtained. The intensities in the difference spectrum may then be used to directly estimate the relative cage occupancies. Three lines are resolved, whose shifts are consistent with single Xe atoms in the cages of the HS-I structure: The shift at 251 ppm corresponds to Xe in the small D ( $5^{12}$ ) cages. The line at 107 ppm has not been seen before, falling between the shifts of Xe in the T ( $5^{12}6^2$ ) cage of sI (at 148 ppm) and the large H ( $5^{12}6^4$ ) cage of sII ( $\approx 79$ –86 ppm), and can logically be assigned to Xe in the P ( $5^{12}6^3$ ) cages.

The third line at 135 ppm, slightly lower than the T ( $5^{12}6^2$ ) cage of sI, can be assigned to the T ( $5^{12}6^2$ ) cage of HS-I.

Analysis of the static and MAS spectra reveals that Xe in the D ( $5^{12}$ ) cage has a CSA, consistent with this cage's symmetry in HS-I. For Xe in the P ( $5^{12}6^3$ ) and T ( $5^{12}6^2$ ) cages, the observation of CSAs, which are zero or very small is also consistent with the HS-I crystal structure, which allows, but does not require CSA.

Integrated signal intensities from Fig. 3E provide relative (but not absolute) cage occupancies for D:T:P of 3.00:1.36:0.91 Xe. Thus, some T and P cages must be empty, because for full occupancy the ratio should be 3:2:2, and the small D cage is not necessarily fully occupied. The NMR numbers are equivalent to 2.394:1.085:0.726 for comparison with the “absolute” X-ray numbers given in Table 1, the 2 methods generally agree on reduced cage occupancies.

## Conclusions

We have observed and characterized using X-ray diffraction and NMR techniques a previously unobserved form of a true clathrate hydrate containing only Xe atoms as guests. This previously unobserved form was produced from an initial pressurization of sI Xe hydrate followed by a temperature quench recovery, from 2.0 GPa at room temperature, to 77 K and ambient pressure. We confirmed reproducibility of the material with 2 samples produced at different times. It is not known whether this form of clathrate is produced as an intermediary between sI and the high pressure sH, or is formed from the high pressure sH as the sample is quench-recovered. It has, however, not been reported from in situ experiments. Nonetheless this structure is shown to exhibit a hexagonal crystal symmetry of the postulated HS-I form, and has a composition very similar to the initial sI hydrate. This hydrate is stable at atmospheric pressure up to 160 K before decomposing to sI hydrate. Static and magic angle spinning Xe NMR data confirm the formation of 3 cage environments entirely consistent with the structure characterized by X-ray data analysis and is consistent with a fairly large degree of oxygen disorder. These data on 2 distinct clathrate hydrate samples with similar composition further illustrate the structural complexity in gas hydrates and indicates that thermodynamic pathways play a critical role in the ultimate determination of hydrate structures.

## Materials and Methods

Xe clathrate hydrate, sI, was first synthesized from powdered ice at the National Research Council of Canada (NRC) Steacie Institute for Molecular Sciences, as outlined in ref. 25. Each of the 2 samples were then quenched to liquid nitrogen temperature and recovered at ambient pressure. This produced several cubic centimeters of pure hydrate sample that was then subdivided for the various experiments reported here. One subsection of each sample was cold loaded (at 77 K) into an indium cup and placed in a piston cylinder large volume high pressure device. Before sealing the indium cup, it was heated to above liquid nitrogen temperature and excess liquid nitrogen was allowed to boil away. The indium cup was then sealed and pressurized to 0.20 ( $\pm 0.05$ ) GPa to stabilize the clathrate and then allowed to warm to 250 ( $\pm 5$ ) K before compression to 1.20 ( $\pm 0.05$ ) GPa at which point the sample was further warmed to 287 ( $\pm 5$ ) K before further increasing the pressure to 2.0 ( $\pm 0.1$ ) GPa. The sample was then temperature quenched in liquid nitrogen and recovered to ambient pressure. The rate of volume change at 2.0 GPa was sensitive to temperature, indicating that the sample was close to the transformation boundary.

These quench-recovered samples were then subdivided and a portion was shipped cold (77 K) along with the sI starting samples to the Advanced Photon Source (APS), Argonne National Laboratory for high energy X-ray scattering studies. The second portion of the pressure quenched sample along with some sI sample was retained at NRC for solid state NMR studies. At the APS the samples were cold loaded into a liquid He cryostat. Again, before data collection the samples were heated to  $>80$  K to remove excess nitrogen from the sample chamber. The samples were then cooled to 40 K for data collection. These X-ray experiments were carried out at the high energy beamline located at sector 11-ID-B, using 115 keV ( $\lambda = 0.137$  Å X-rays). A MAR 345 detector was located at 700.2 mm, this distance enabled increased resolution at the expense

of momentum transfer range for the Rietveld analysis. Scattering data were collected over a momentum transfer range from 0.25 to  $11 \text{ \AA}^{-1}$ . Laboratory X-ray diffraction (XRD,  $\text{Cu } K\alpha$ ) to determine the decomposition path for the quench-recovered form was carried out at the Center for Nanophase Materials Sciences, Oak Ridge National Laboratory and at the National Research Council Canada.

For the in situ measurements the unpressurized sl form of the hydrate was cold loaded into a DAC at Stony-Brook University. These samples were loaded under cold nitrogen gas. A small pressure of 1.7 GPa was applied to the diamonds so that the sample could be warmed to room temperature without hydrate decomposition. The samples were then mounted on the high energy diffractometer at sector 1 at the APS sector 1-ID. Structural studies of the in situ high pressure form were performed using 80.7 keV,  $\lambda = 0.1537 \text{ \AA}$  X-rays. The initial structure at 1.7 GPa is shown to be that of sl. Subsequently, data were collected at 2.0, 2.6 and 3.5 GPa and the sample transformed to the high pressure sH followed by decomposition into solid Xe and ice VII. The standard Ruby fluorescence scale was used to determine the pressure.

Static  $^{129}\text{Xe}$  NMR spectra with  $^1\text{H}$  cross-polarization and decoupling were obtained at 110.64 MHz on a Bruker DSX-400 spectrometer at the National Ultra-high-Field NMR Facility for Solids and the NRC NMR center at the National

Research Council of Canada. Please see the SI for details about  $^{129}\text{Xe}$  NMR spectra. For spectra at 77 K, samples of the original sl Xe hydrate and the quench-recovered material were loaded into thin-walled 5-mm glass tubes at 77 K in a bath of liquid nitrogen and transferred into the NMR probe (Morris Instruments Inc.), which was precooled. The sample was maintained at 77 K, using liquid nitrogen surrounding the NMR coil. A series of spectra of the quench-recovered sample were obtained at different cross-polarization times ranging from 0.25 ms to 15 ms. Subsequently, spectra were obtained at the optimum cross polarization (CP) time of 3 ms. Static CP and CP/MAS spectra were also obtained at a nominal temperature of 153 K, using a Bruker BL7 MAS probe with 7-mm  $\text{ZrO}_2$  stretched spinners. Chemical shifts were referenced to the gas phase at zero pressure, using Xe-quinol clathrate as the secondary reference (isotropic chemical shift at 222ppm).

**ACKNOWLEDGMENTS.** Oak Ridge National Laboratory is managed by UT-Battelle, LLC for the U. S. Department of Energy under Contract DE-AC05-00OR22725. This work was supported by the scientific user facilities division of DOE-BES at the Spallation Neutron Source (C.A.T., L.Y., and B.C.C.) and Center for Nanophase Materials Science (L.Y.) at Oak Ridge National Laboratory; and the National Science Foundation Grant DMR-0800415 (to C.D.M., L.E., and J.B.P.).

1. Jeffrey GA (1996) in *Comprehensive Supramol Chem*, eds Atwood JL, Davies JED, MacNicol DD, Vogtle F, Lehn JM (Pergamon, New York) Vol 6, Chap 23.
2. Ripmeester JA, Tse JS, Ratcliffe CI, Powel BM (1987) A new clathrate hydrate structure. *Nature* 325:135–136.
3. Udachin KA, Ratcliffe CI, Enright GD, Ripmeester J A (1997) Structure H hydrate: A single crystal diffraction study of 2,2-dimethylpentane 5(Xe,H<sub>2</sub>S). 34H<sub>2</sub>O. *Supramol Chem* 8:173–176.
4. Lu H, et al. (2007) Complex gas hydrate from the Cascadia margin. *Nature* 445:303–306.
5. Ripmeester JA, Ratcliffe CI, Klug DD, Tse JS (1994) Molecular perspectives on structures and dynamics in clathrate hydrates. *Annal New York Acad Sciences* 715:161–176.
6. Manakov AY, et al. (2004) Structural Investigations of argon hydrates at pressures up to 10 kbar. *J Inclusion Phenom Macrocyclic Chem* 48:11–18.
7. Ogienko AG, et al. (2006) Gas hydrates of argon and methane synthesized at high pressures: Composition, thermal expansion, and self-preservation. *J Phys Chem B* 110:2840–2846.
8. Loveday JS, Nelmes RJ, Klug DD, Tse JS, Desgreniers S (2003) Structural systematics of clathrate hydrates under pressure. *Can J Phys* 81:539–544.
9. Loveday JS, et al. (2001) Stable methane hydrate above 2 GPa and the source of Titan's atmospheric methane. *Nature* 410:661–663.
10. Hirai H, Machida S, Kawamura T, Yamamoto Y, Yagi T (2006) Stabilizing of methane hydrate and transition to a new high-pressure structure at 40 GPa. *Am Mineral* 91(5–6):826–830.
11. Dyadin YA, Belosludov VR (1996) in *Comprehensive Supramol Chem*, eds Atwood JL, Davies JED, MacNicol DD, Vogtle F, Lehn JM (Pergamon, New York,) Vol 6, Chap 24.
12. Loveday JS, Nelmes RJ, Guthrie M, Klug DD, Tse JS (2001) Transition from cage clathrate to filled ice: The structure of methane hydrate III. *Phys Rev Lett* 87:215501.
13. Loveday JS, Nelmes RJ, Guthrie M (2001) High-pressure transitions in methane hydrate. *Chem Phys Lett* 350:459–465.
14. Sasaki S, Hori S, Kume T, Shimizu H (2003) Microscopic observation and in situ Raman scattering studies on high-pressure phase transformations of a synthetic nitrogen hydrate. *J Chem Phys* 118:7892–7897.
15. Sanloup C, Mao H-k, Hemley RJ (2002) High pressure transformation in xenon hydrates. *Proc Natl Acad Sci USA* 99:25–28.
16. Udachin KA, Ratcliffe CI, Enright GD, Ripmeester JA (2008) Transformation of the hexagonal-structure clathrate hydrate of cyclooctane to a low-symmetry form below 167K. *Angew Chem Int Ed* 47:9704–9707.
17. Panke D (1968) The structure of 4(CH<sub>3</sub>)<sub>3</sub>N. 41H<sub>2</sub>O. *J Chem Phys* 48:2990–2996.
18. Kosyakov VI, Shestakov VA, Solodovnikov SF (1994) Calculation of the gas hydrate HS-1 framework structure and its energy estimation. *J Struct Chem* 34(5):810–813.
19. Udachin KA, Enright GD, Ratcliffe CI, Ripmeester JA (1997) Structure, stoichiometry, and morphology of bromine hydrate. *J Am Chem Society* 119:11481–11486.
20. Vatamanu J, Kusalik PG (2006) Unusual crystalline and polycrystalline structures in methane hydrates. *J Am Chem Soc* 128:15588–15589.
21. Alavi S, Ripmeester JA, Klug DD (2006) Stability of rare gas structure H clathrate hydrates. *J Chem Phys* 125:104501.
22. Syassen K, Holzapfel W (1978) High pressure equation of state of solid Xe. *Phys Rev B* 18:5826–5834.
23. Ripmeester JA, Ratcliffe CI, Tse JS (1988) The NMR of  $^{129}\text{Xe}$  trapped in clathrates and some other solids. *J Chem Soc Faraday Trans* 84:3731–3745.
24. Ripmeester JA, Ratcliffe CI (1990)  $^{129}\text{Xe}$  NMR study of clathrate hydrates: New guests for structure II and structure H. *J Phys Chem* 94:8773–8776.
25. Handa YP (1986) Calorimetric determination of the compositions, enthalpies of dissociation, and heat capacities in the range 85 to 270 K for clathrate hydrates of xenon and krypton. *J Chem Thermodyn* 18:891–902.